International Journal of Pharmaceutics 406 (2011) 1–10

Contents lists available at ScienceDirect

International Journal of Pharmaceutics

journal homepage: www.elsevier.com/locate/ijpharm

Review

Influence of particle size on regional lung deposition – What evidence is there?

Thiago C. Carvalho[a], Jay I. Peters[b], Robert O. Williams III[a,*]

[a] Division of Pharmaceutics, College of Pharmacy, University of Texas at Austin, Austin, TX, USA
[b] Department of Medicine, Division of Pulmonary Diseases/Critical Care Medicine, The University of Texas Health Science Center at San Antonio, San Antonio, TX, USA

ARTICLE INFO

Article history:
Received 6 October 2010
Received in revised form
22 December 2010
Accepted 27 December 2010
Available online 11 January 2011

Keywords:
Inhalation therapy
Regional lung deposition
Particle size distribution
Aerodynamic diameter
Imaging techniques

ABSTRACT

The understanding of deposition of particles in the respiratory tract is of great value to risk assessment of inhalation toxicology and to improve efficiency in drug delivery of inhalation therapies. There are three main basic mechanisms of particle deposition based primarily on particle size: inertial impaction, sedimentation and diffusion. The regional deposition in the lungs can be evaluated in regards to the aerodynamic particle size, in which particle density plays a significant role. In this review paper, we first introduce the available imaging techniques to confirm regional deposition of particles in the human respiratory tract, such as planar scintigraphy, single photon emission computed tomography (SPECT) and positron emission tomography (PET). These technologies have widely advanced and consequently benefited the understanding of deposition pattern, although there is a lack of lung dosimetry techniques to evaluate the deposition of nanoparticles. Subsequently, we present a comprehensive review summarizing the evidence available in the literature that confirms the deposition of smaller particles in the smaller airways as opposed to the larger airways.

Contents

1. Introduction

Particles are deposited in the respiratory tract when they are removed in a definitive fashion from the flow streamline generated by the breathing maneuver. Understanding this process and the factors influencing particles settlement in the surface of specific regions of the airway tree has implications to the development of pharmaceutical inhalation products for aerosol therapy and to risk assessment of air pollutants that concerns toxicology.

Besides pulmonary physiology of patients (e.g. breathing pattern and lung geometry), particle deposition is also known to be influenced by aerosol characteristics (Gonda, 2004; Zeng et al., 2001). Namely, the physicochemical properties of inhaled aerosols that can determine deposition are: size, size distribution, shape, charge, density and hygroscopicity (Pilcer and Amighi, 2010). In the field of aerosol medicine, particle size is a formulation design variable that can be engineered accordingly, aiming the development of pulmonary drug delivery systems (Chow et al., 2007; Shoyele

* Corresponding author.
E-mail address: williro@mail.utexas.edu (R.O. Williams III).

0378-5173/$ – see front matter © 2011 Elsevier B.V. All rights reserved.
doi:10.1016/j.ijpharm.2010.12.040

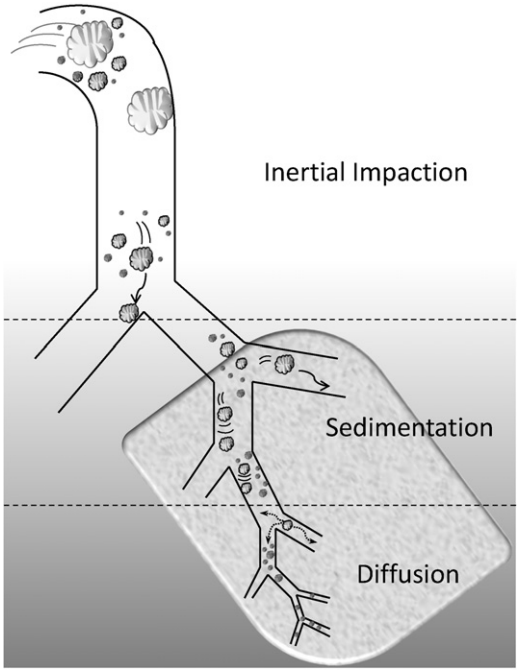

Fig. 1. Schematic diagram representing particle deposition in the lungs according to different mechanisms related to particle size: inertial impaction, sedimentation and diffusion. The diagram presents the smaller particles depositing in the lower airways as opposed to the larger airways. The GI tract is omitted in this diagram.

and Cawthome, 2006). As we can examine from the mechanisms of deposition, particle diameter is the primary factor determining pulmonary deposition of aerosols in the various regions of the respiratory tract. Ultimately, inspiratory flow rate also plays an important role in the particle deposition following pulmonary administration (Dolovich, 2000).

In this review paper, we summarize the evidence available in the literature to confirm that smaller particles delivered to the lungs are deposited in the smaller airways as opposed to the larger airways (Fig. 1). So, we first present the mechanisms of particle deposition and the relevance of particle aerodynamic diameter for regional lung deposition. Following, we present experimental techniques that can be used to confirm regional deposition of particles in the respiratory tract. Our focus herein is on evidence of deposition patterns applied to inhalation therapies in humans, based on available data about particle aerodynamic size.

2. Mechanisms of particle deposition

There are five different mechanisms by which particle deposition can occur in the lungs: inertial impaction, sedimentation, diffusion, interception and electrostatic precipitation. The two latter mechanisms are related, respectively, to particle shape (e.g. elongated particles) and electrostatic charges; and have been reviewed in detail elsewhere (Gonda, 2004; Zeng et al., 2001). The mechanisms of deposition directly (or inversely) related to particle size are presented in Fig. 2.

2.1. Inertial impaction

Inertial impaction occurs when airborne particles possess enough momentum to keep its trajectory despite changes in direction of the air stream, consequently colliding with the walls of the respiratory tract. The chances of deposition by impact are increased when the particles are more likely to travel longer distances, *S*, which is based on the particle mobility (velocity per unit force),

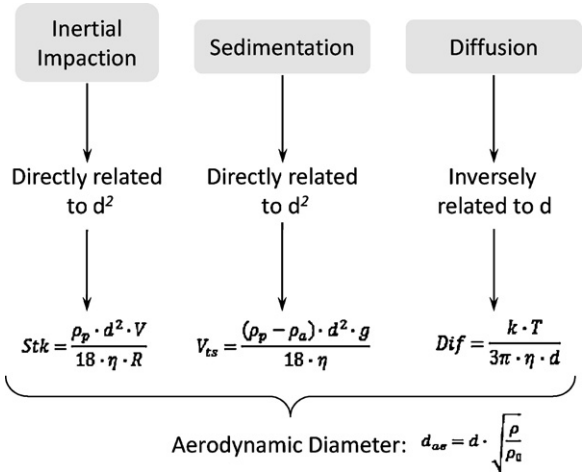

Fig. 2. The influence of particle size on deposition. *d*: particle diameter; *Stk*: Stokes number; ρ_p: particle density; *V*: air velocity; η: air viscosity; *R*: airway radius; V_{ts}: terminal settling velocity; ρ_a: air density; *g*: gravitational acceleration; *Dif*: diffusion coefficient; *k*: Boltzmann's constant; *T*: absolute temperature; d_{ae}: aerodynamic diameter; ρ_0: unity density.

B, mass, *m*, and velocity, *v*, according to Eq. (1) (Gonda, 2004):

$$S = B \cdot m \cdot v \tag{1}$$

The dimensionless Stokes' number, *Stk*, more specifically describes the probability of particle deposition in the airways via impaction. The higher the Stokes' number, the more readily particles will be deposited by inertial impaction, according to Eq. (2):

$$Stk = \frac{\rho_p \cdot d^2 \cdot V}{18 \cdot \eta \cdot R} \tag{2}$$

where ρ_p is the particle density, *d* is the particle diameter, *V* is the air velocity, η is the air viscosity and *R* is the airway radius. Therefore, considering the bifurcated architecture of the lungs, large particles travelling through the airways at high airflow velocity are more likely to impact in the proximal portion of the respiratory tract (upper airways) (Zeng et al., 2001).

2.2. Sedimentation

Sedimentation is a time-dependent process in which particles settle due to the influence of gravity. Hence, breathing maneuvers in which more time is allowed for the particles to sediment (e.g. breath-holding) may increase lung deposition (Zeng et al., 2001). The Stokes' Law assumes that the relative velocity between the surface of the particle and the airstream is null. Considering unit density spheres of 1–40 μm, Stokes' law can be used to predict the terminal settling velocity, V_{ts}, according to Eq. (3):

$$V_{ts} = \frac{(\rho_p - \rho_a) \cdot d^2 \cdot g}{18 \cdot \eta} \tag{3}$$

where ρ_a is the density of air ($\rho_p > \rho_a$) and *g* is the gravitational acceleration (Gonda, 2004). However, for particles smaller than 10 μm, a slip correction factor (C_c) derived by Cunningham should be applied to Stokes' law, as described in Eq. (4) (Crowder et al., 2002).

$$C_c = 1 + Kn \cdot \left[A_1 + A_2 \cdot \exp\left(-\frac{A_3}{Kn}\right)\right] \tag{4}$$

where *Kn* is the Knudsen Number, and A_1, A_2 and A_3 are constants. The size-dependence of this equation is related to the balance between the downward force exerted by the particle and the resistant force for which Stokes' law is valid. With increased air flow, the stream becomes turbulent and the deposition by impaction

increases (Zeng et al., 2001). Therefore, this equation assumes laminar flow within the airways, as defined by the Reynolds number, R_e (Eq. (5)).

$$R_e = \frac{\rho_a \cdot V \cdot d}{\eta} \quad (5)$$

Interestingly, the effect of gravity on particle sedimentation has recently been evaluated by the National Aeronautics and Space Administration (NASA). Inhalation of lunar dust is a concern for potential toxicological effects to future explorers of the moon (Darquenne and Prisk, 2008). Six healthy subjects were administered aerosols with particle diameters of 0.5 and 1.0 μm on the ground (1 g) and during short periods of lunar gravity (1/6 g). In this study, the researchers found that, although the deposition of fine particles is greater on earth, peripheral deposition was improved at low gravity for those particles that are actually deposited in the lunar environment.

2.3. Diffusion

Diffusion occurs when particles are sufficiently small to undergo a random motion due to molecular bombardment. This process, also known as Brownian motion, is correlated to particle size, according to Stokes–Einstein equation (Eq. (6)) (Gonda, 2004):

$$Dif = \frac{k \cdot T}{3\pi \cdot \eta \cdot d} \quad (6)$$

where *Dif* is the diffusion coefficient, k is the Boltzmann's constant and T is the absolute temperature. Different from impaction and sedimentation mechanisms, diffusional deposition is therefore inversely related to particle size.

3. Particle aerodynamic diameter

Aerosols for inhalation vary not only on geometric particle size and size distribution, but also in a number of other factors that influence particle deposition: physical state (liquid or solid), density, shape and velocity. In addition, a dynamic system of forces is interacting with the airborne particles throughout the airways, namely: gravity, resistant force of the inspiratory air and inertial force. The balance between these forces and the aerosol properties ultimately determines the mechanism of particle deposition in the lungs (de Boer et al., 2002).

The aerodynamic diameter, d_{ae}, is, by definition, the diameter of a sphere with unit density ($\rho = 1$), having the same terminal settling velocity in still air as the particle in consideration (de Boer et al., 2002). Considering the particle characteristics, this independent variable can therefore correlate the effect of geometric diameter and particle density, as described in Eq. (7):

$$d_{ae} = d \cdot \sqrt{\frac{\rho}{\rho_0}} \quad (7)$$

where d is the actual diameter of the sphere, ρ is the spherical particle density and ρ_0 is unit density. For non-spherical particles, which are more prone to deposition via interception, the particle shape also influences the aerodynamic diameter and therefore correction for shape factors are applied (Gonda, 2004; Zeng et al., 2001).

The relationship between the geometric diameter and the particle density for aerodynamic diameter is illustrated by a study of large porous particles for pulmonary delivery (Edwards et al., 1997). In this investigation, Edwards et al. have effectively delivered very light weight large particles ($\rho = 0.1$ g/cm^3; $d = 8.5$ μm) to the deep lung. Therefore, aerodynamic diameter, as opposed to geometric diameter, must be used as independent variable to relate to particle deposition governed primarily by inertial impaction (Mitchell and Nagel, 2003). *In vitro* determination of the aerodynamic size of inhalation products can be performed by cascade impactors, including Andersen Cascade Impactors, Multi-Stage Liquid Impinger and Next Generation Cascade Impactors (de Boer et al., 2002). This characterization is essential to evaluate the particle deposition in the lungs. Usually, the mass median aerodynamic diameter (MMAD) and the geometric standard deviation (GSD) are reported. MMAD is the cut off particle size in which 50% of the mass of the aerosol is smaller and the other 50% is larger than the referred parameter (Jaafar-Maalej et al., 2009). MMAD is a measure of central tendency while GSD indicates the magnitude of dispersity from the MMAD value (Pilcer et al., 2008).

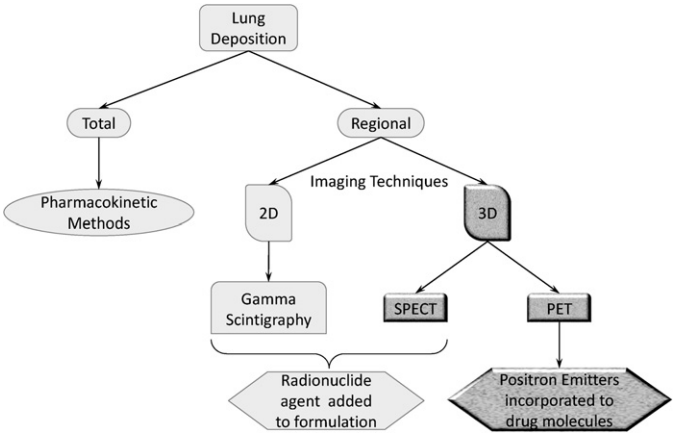

Fig. 3. Commonly used methods for assessment of regional lung deposition. 2D: two-dimensional; 3D: three-dimensional; SPECT: Single Photon Emission Computed Tomography; PET: Positron Emission Tomography.

During the inhalation process of pharmaceutical products, a specific device is positioned in the mouth of the patients and the drug particles are aerosolized. These particles travel throughout the airways with a number of factors determining its deposition in the respiratory tract, which can be anywhere from the oral cavity to the alveoli. There are a number of mathematical models and computational tools available in the literature that aids in predicting the deposition patterns of particles in the whole lung and in its specific regions, even considering different disease states. These topics have recently been reviewed and beyond the scope of this review (Balashazy et al., 2007; Kleinstreuer et al., 2008; Martonen et al., 2003; Rostami, 2009).

4. Assessment of regional lung deposition

An overview of the commonly used techniques is presented in Fig. 3. There are two basic methods to identify drug deposition in the lungs following inhalation: pharmacokinetic methods and gamma-scintigraphy techniques (Cryan et al., 2007). The former one can only provide information about total lung dose, based on plasma concentrations and/or urinary recovery (Chrystyn, 2001; Koehler et al., 2003). On the other hand, besides quantifying total lung deposition, radionuclide imaging (or gamma-scintigraphy) is the primary technology used to differentiate between depositions into different zones of human lungs (Moller et al., 2009b). This *in vivo* imaging technology is greatly valued due to its ability to provide visual confirmation (and therefore convincing evidence) that the dosage form is functioning in the way it is designed to, by demonstrating that the drug particles are being deposited into the lungs following inhalation. Initially, two-dimensional gamma-scintigraphy was used as imaging technique for delivery of inhaled drugs. Lately, tridimensional imaging technologies have been applied for more accurate particle deposition in the human respiratory tract, including single photon emission com-

puted tomography (SPECT) and positron emission tomography (PET). More recently, a new experimental technique based on magnetic resonance imaging (MRI) has been published and is herein discussed briefly.

4.1. Two-dimensional gamma scintigraphy

This planar imaging technique has been extensively used to assess the delivery efficiency of inhaled drugs (Davis et al., 1992; Newman, 1993), in which deposition patterns can be determined for different formulations and devices used for pulmonary administration. Usually, the radiolabelling process involves adsorbing the imaging agent to the surface of the drug particle (Newman et al., 2002) or adding the radionuclide to the nebulizer solution (Coates et al., 2008; Schmekel et al., 2002). The radionuclide Technetium (^{99m}Tc, half life of 6 h) has been widely utilized as radiolabelling agent for imaging of structure and function of different organs (Clark et al., 2008). Other radionuclides include ^{111}In, ^{123}I and ^{67}Ga (Newman et al., 2003). Mucociliary clearance, coughing and rapid permeability of the tracer through the airways limit the process to a short period of time when evaluating particle deposition patterns (Chrystyn, 2001). Despite this, accurate quantification of particle deposition in the lungs can be obtained, as long as drug and radionuclide distributions for comparative particle size ranges are equivalent and the radiolabelling process does not affect the particle size distribution of the drug (Farr, 1996).

Gamma scintigraphy operates with either a single-headed or dual-headed gamma camera positioned to take static images. When fitted into a two-dimensional perspective these images can provide information about the distribution of the radiolabelling agent in the organ of interest (Newman and Wilding, 1999). To determine the specific region at which particles are deposited onto the lung using gamma scintigraphic methods, it is common practice to spatially divide the lungs into sections of interest (e.g. central, intermediate and peripheral) using computer tools. Based on the regions of interest, the Peripheral to Central (P/C) ratio (or, inversely, the Central to Peripheral C/P ratio) of particle deposition is widely used as planar index (Chrystyn, 2001; Newman et al., 2003). In this image division, the peripheral zone refers mainly to the small airways ($\leq$2 mm) while the central portion of the lung represents the larger airways. Hence, the P/C ratio correlates to the proportion of drug particles deposited in the respiratory bronchiole/alveolar region as compared to tracheobronchial regions of the lung.

One of the main drawbacks of the planar scintigraphy though is the projection of the (three-dimensional) lung structure into a two-dimensional image. Relative particle deposition at different plane levels of the lungs may obscure the real deposition pattern when using this technique. Consequently, the lack of three-dimensional resolution can cause overestimation of deposition due to overlapping airways. Based on a coronal position image, this effect is considerably higher in the hilar region and gradually decreases towards the small airways in the periphery. Hence, it has been highly recommended to correct for attenuation of the radioactivity in the chest wall (Dolovich, 2000; Moller et al., 2009a). To overcome this issue, SPECT and PET provide information about three-dimensional intrapulmonary deposition pattern that can reduce this source of error.

4.2. Single photon emission computed tomography (SPECT)

With the gamma camera rotating through 360°, SPECT provides three-dimensional image of the lungs (Chrystyn, 2001). Similar to gamma scintigraphy, the single-headed cameras rotate around the chest of the patient laid in supine position. However, with single detector cameras the scanning time can be unacceptably long (e.g. greater than 15 min), since relative quantification can be erroneous due to significant absorption, mucociliary clearance (1 mm/min), or cough (Berridge et al., 2000b; Chan et al., 1999). For this reason, twin-headed or even triple-headed cameras have been used to boost analysis efficiency.

Using the same radiolabelling method as in gamma scintigraphy, the obtained scans can be used to reconstruct the three-dimensional distribution of the particles in the lungs using an algorithm (Newman et al., 2003). SPECT can then be used to determine regional lung deposition by differentiating between small and large airways (Eberl et al., 2006). As opposed to planar sections (based on pixels), the lung structure can be divided into volumes of interest, also known as voxels. For instance, in one of these techniques, the airway tree is arbitrarily divided into lung layers in the shape of concentric "shells" with the main bronchial bifurcation as the reference point (Berridge et al., 2003; Fleming et al., 1997). Based on gamma camera counts, these shells are further converted into spatial distributions that can consequently be used in the definition of Penetration Index (PI = P/C or C/P ratio). Given the arbitrary definition of this index established according to the research group, they should be analyzed on a case-by-case basis.

More recently, the development of 3D *in silico* models that can be superimposed on laboratory images of SPECT and PET may improve the interpretation of regional particle deposition in the lungs from clinical data (Martonen et al., 2005, 2007). In this manner, the individual anatomy is preserved and, based on the airway dimensions of a lung model; the airway generation contribution to each shell can be detailed. Unquestionably, such 3D *in silico* model is a powerful tool to better elucidate regional particle deposition patterns in the airways.

4.3. Positron emission tomography (PET)

While in SPECT the formulation is radiolabelled with surrogate markers like ^{99m}Tc, PET incorporates positron emitters such as ^{11}C and ^{18}F into the drug molecule (Chrystyn, 2001; Newman et al., 2003; van Waarde et al., 2005). Although the radiolabelling method in PET is considerably more elaborated, some drugs have been used for PET studies as aerosols, including: ^{11}C-triamcinolone (Berridge et al., 2000a), ^{11}C-formoterol (Visser et al., 1998), ^{18}F-insulin (Guenther et al., 2006), ^{124}I-insulin, and ^{125}I-insulin (Iozzo et al., 2002). Alternatively, the lung physiology can be studied by using aerosols of ^{18}F-Fluorodeoxyglucose (FDG – Dolovich, 2009). The need to formulate the radiolabelled drug into an inhaled dosage form (e.g. dry powder) and further load it into the respective delivery device (e.g. dry powder inhaler) requires consideration of the isotope decay from the time the radiolabelling process is finished. This procedure can be very challenging when considering the short half lives of these radionuclides: 20 min for ^{11}C and 110 min for ^{18}F (Dolovich and Labiris, 2004).

In studying pulmonary deposition based on particle size, changes in the physicochemical properties of the particles due to the addition or incorporation of the radionuclide into the drug molecule or formulation may occur. Therefore, a verification that the particle size distribution after introduction of the tracer into the formulation has not changed significantly is required (Berridge et al., 2003). For instance, an investigation of budesonide delivered with pressurized Metered Dose Inhaler (pMDI), pMDI with Nebuhaler®, a large volume spacer, and Turbuhaler®, a dry powder inhaler (DPI) in eight asthmatic patients using gamma scintigraphy showed a P/C ratio of 1.24, 1.22 and 0.64, respectively (Thorsson et al., 1998). Despite the increased peripheral deposition of the pMDI device, however, the incorporation of ^{99m}Tc tracer to the formulation did not present similar sizes before and after the

radiolabelling process. In this case, underestimation of particle deposition may have occurred.

4.4. Magnetic resonance imaging (MRI)

More recently, a MRI method of measuring regional lung deposition has been published based on superparamagnetic iron oxide nanoparticles (Martin et al., 2008). The feasibility of this method was demonstrated in a study where mice were administered colloidal suspensions of the nanoparticles via a nose-only inhalation chamber. The MMAD of the aerosol droplets formed using a Pari LC Star® jet nebulizer was 5.6 ± 0.8 μm, with a geometric standard deviation (GSD) of 1.30 ± 0.03 ($n = 6$), as measured by time-of-flight technique (Shekunov et al., 2007). The longitudinal relaxation time of 12 axial slices of the lungs was analyzed using MRI and subsequently converted to iron concentration. The methodology showed potential for analysis of regional lung deposition, resulting in greater concentration of iron in central regions of the mice lungs. This is an expected result, based on MMAD value, as it is discussed in more details in the next section. As such, this technique has a potential as an alternative for scintigraphic methods for determining deposition patterns in the various regions of the lungs. Additionally, this experimental technique also shows considerable promise for evaluation of magnetic-based formulations for pulmonary drug delivery, in which particles are already loaded with iron oxide (Xie et al., 2010).

5. Particle deposition in the lungs

Stahlhofen and coworkers have previously studied the effect of particle size on lung deposition in a systematic experimental design with subjects inhaling monodisperse aerosols during tidal breathing (Stahlhofen et al., 1989). With a tube inserted into the mouth, the oropharyngeal (mouth and throat) deposition for particles greater than 10 μm was more than 90% and 50% at 60 and 18 L/min, respectively. In their study, the smaller airways were differentiated by the larger airways according to the time of particle clearance from the lungs based on scintigraphic methods. A "fast-cleared" fraction was correlated to lung deposition at the tracheobronchial region (or larger airways), attributed to the known mechanism of mucociliary clearance in this area. Alternatively, a "slow-cleared" fraction was correlated to the absence of cilia in the terminal portion of the airway, indicating deposition in the lower airways and an expected particle clearance at approximately one day. By subtracting the slow-cleared fraction observed after a period of about 24 h from the initial total lung dose, the regional deposition of particles is determined (Finlay, 2001). According to this experimental design and with particle aerodynamic diameter measured at an airflow rate of 30 L/min, it was found by Stahlhofen et al. that particles of approximately 6 and 3 μm are deposited predominantly in the larger and smaller airways, respectively. Notably a high inter-subject variability was observed (Stahlhofen et al., 1989). These results are in agreement with the particular mechanisms of deposition: inertial impaction and sedimentation. Interestingly, it was also found in this study that as particle sizes decrease to submicron dimensions the total lung deposition also decreased. With further decrease in particle size into the nanometric scale, the total lung deposition increased back to levels equivalent or greater than micronized particles (Fig. 4). This minimum of total lung deposition may be attributed to a crossover between predominance of diffusion versus impaction/sedimentation mechanisms based on their particle sizes (Finlay, 2001).

Similar studies in terms of experimental design are reported in the literature (Meyer et al., 2003). However, there is evidence supporting that some particles depositing in the tracheobronchial region are actually cleared slowly and independent on their geometric diameters (Smith et al., 2008). Therefore, the accuracy in determining regional pulmonary deposition from different particle sizes based on particle clearance should be evaluated with caution.

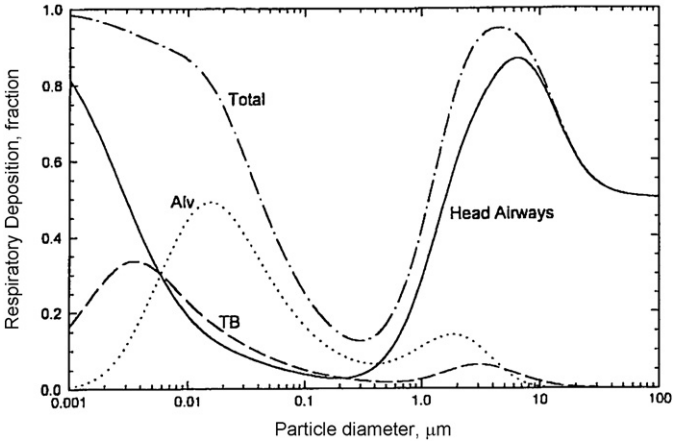

Fig. 4. Average predicted total and regional lung deposition based on International Commission on Radiological Protection (ICRP) deposition model for nose breathing males and females engaged in light exercise. Alv: alveolar region; TB: tracheobronchial region.
Source: Figure reprinted with permission from Hinds (1999).

Early on, evidence about the deposition of smaller particles in the smaller airways also emerged from related therapeutic response. According to the pathophysiology of asthma, inflammation may occur throughout the entire airway. Given the easy accessibility of the large airways, early studies related to this chronic inflammation had been done in the proximal central region, neglecting the occurrence in the distal airways (Carroll et al., 1993). In a series of studies, Zanen and coworkers demonstrated a significant improvement in lung function of stable asthma patients may be influenced by disease severity as well as particle characteristics. In the first study, monodisperse solutions of ipratropium bromide were aerosolized to mild asthma patients, with MMADs of 1.5, 2.8 and 5.0 μm and GSDs smaller than 1.2 (Zanen et al., 1995). Improvement in forced expired volume was observed for patients inhaling equivalent doses of aerosols with MMADs of 1.5 and 2.8 μm only. Following this study, monodisperse salbutamol or ipratropium bromide solutions were administered in equal doses to asthma patients with severe obstruction (Zanen et al., 1996). For aerosols with the same aerodynamic characteristics as in the previous study, only particles with MMADs of approximately 3 μm presented improvement in the respiratory tract in this subset of patients. Not able to visualize the deposition patterns with imaging techniques, the authors were unable to explain why the aerosol with small particles (MMAD of 1.5 μm) presented similar lung function improvement as the solution aerosolized presenting larger particles (MMAD of 5.0 μm). These data suggest that aerodynamic diameter, geometric standard deviation and the degree of underlying airway disease may all impact the delivery as well as the therapeutic response to inhaled medications. Finally, Zanen et al. compared the monodisperse ipratropium bromide aerosol (MMAD 2.8 μm; GSD 1.1) with a polydispersed pMDI formulation of the same drug (MMAD 1.8; GSD 2.0) (Zanen et al., 1998). The wide distribution of particle sizes of the pMDI formulation was found to be not as efficacious as the monodisperse delivery of the aerosol, based on lung function improvement. Subsequent studies have found that inflammation at distal portions of the lungs play a significant role in development and persistence of asthma symptoms (Martin, 2002).

More evidence for the deposition of smaller particles in the lower airways occurred after chlorofluorocarbons (CFC) were man-

dated to be removed from pMDIs, according to the 1987 Montreal Protocol on Substances that Deplete the Ozone Layer (UNEP, 1987). Gradually, the propellant CFC was being phased out and substituted by hydrofluoroalkanes (HFA), given its safety profile (Emmen et al., 2000). The need for reformulation provided the opportunity to produce solutions of inhaled corticosteroids (e.g. flunisolide and beclomethasone) with the propellant HFA, as opposed to the then available CFC-based suspensions (Corren and Tashkin, 2003; Vanden Burgt et al., 2000). The HFA-based formulation of beclomethasone dipropionate (QVAR®) was able to produce aerosols with MMADs of 1.1–1.2 μm, much smaller aerodynamic particle sizes than the CFC-based formulations with MMADs varying from 3.5 to 4.0 μm. Several studies comparing QVAR® and CFC-based formulations were performed for inhaled corticosteroids like beclomethasone and flunisolide (Corren and Tashkin, 2003; Leach et al., 1998; Leach et al., 2005). The deposition patterns were based on percentage of ^{99m}Tc radiolabelled particles deposited in the oropharyngeal cavity (upper airways) versus the deposition in the deep lung (lower airways). The smaller aerodynamic particles of the HFA-based solution formulation were consistently deposited in the deep lungs in a considerably higher proportion than with the CFC-based suspension formulations. Such findings have not been consistent with all HFA formulations though. Scintigraphic studies for beclomethasone and flunisolide HFA show dramatically increased lung deposition (50–70%) when compared to CFC formulations (5–20%) (Martin, 2002). The increased solubility in HFA for some drugs is likely the reason for smaller particle size. The importance of solubility on the particle size is illustrated by the scintigraphic studies of mometasone furoate HFA. Unlike the HFA-soluble drugs beclomethasone and flunisolide, mometasone furoate is currently delivered in an aerosol suspension. Studies by Pickering et al. demonstrated lung deposition of mometasone furoate HFA of approximately 14% for a formulation presenting only approximately 20% of particles smaller than 5.8 μm (Pickering et al., 2000). Thus, in evaluating the reduction in particle size with HFA-based formulations, one must take into account drug solubility. Therefore, the relatively low lung deposition of mometasone furoate HFA has been shown to be similar to the CFC-based suspension formulations. Importantly, both present larger particle sizes than the HFA-based solution formulations.

pMDIs represent a high ballistic effect when actuated and therefore the particles are more prone to deposit via inertial impaction (Labiris and Dolovich, 2003). On the other hand, aerosols generated by nebulizers may be more dependent on the breathing pattern of patients (Gurses and Smaldone, 2003). Sangwan and coworkers have investigated the regional deposition patterns from aerosols generated by Misty-Neb® (MMAD = 3.1 μm) and AeroEclipse® (MMAD = 2.2 μm) (Sangwan et al., 2003). The total lung deposition measured by two-dimensional scintigraphy was two-fold smaller for the aerosols with larger particle size, and therefore presented a proportional increase in oropharyngeal deposition. The peripheral deposition though was higher for the aerosols generated from Misty-Neb®, with a C/P ratio of 1.5 as compared to 1.9 for AeroEclipse®. This controversial finding was attributed to the relatively extended time required for nebulization with the breath-actuated nebulizer AeroEclipse® (20 min). As discussed earlier, the use of single-headed SPECT presents the disadvantage of long scanning times, allowing for particle clearance to occur. In the same manner, the effect of extended time due to aerosol generation may have hindered the evidence of small particles depositing in the alveoli. Nevertheless, the evidence that the larger particles were deposited in the upper airways was confirmed.

Also using planar gamma-scintigraphy, an evaluation of the regional deposition of monodisperse particles was performed in twelve asthma patients in a more recent study (Usmani et al., 2005). Albuterol was radiolabelled with ^{99m}Tc and aerosolized using a spinning-disk aerosol generator able to provide a GSD smaller than 1.22. For regional deposition analysis, the lung images were divided in three different zones: central, intermediate and peripheral. The penetration index (P/C ratio) results for particles with MMADs of 1.5, 3.0 and 6.0 μm were 0.79, 0.60 and 0.36, respectively. When considering central and intermediate zones together, the percentage of deposition in the peripheral lung zone compared to the total lung dose was still high for smaller particles: 44, 34 and 25%, respectively. The increase in penetration index values with decreasing particle sizes observed in this study clearly confirms the deposition of smaller particles in the smaller airways (peripheral lung region). On the other hand, larger particles are more likely to deposit in the upper airways that present a larger caliber. The deposition pattern of monodispersed particles with aerodynamic diameters of 1, 2.75 and 4.75 μm were reported likewise in another study (Brand et al., 1999). In this investigation, 90% of the larger particles (MMAD 4.75 μm) were deposited in the upper airways. Also, increase in airflow rate demonstrated the effect of inertial impaction in larger particles, by increasing deposition in the upper respiratory tract.

With the advances in SPECT instrumentation, multi-headed cameras have been used to decrease the image acquisition time and provide more reliable regional deposition patterns in the lungs. Eberl and coworkers have introduced a dynamic SPECT technique in which acceptable image quality was obtained with 2-min frame using a triple-detector gamma camera (Brand et al., 1999; Chan et al., 2002; Eberl et al., 2001). In this study, the investigators compared the sensitivity of planar scintigraphy data with fast acquisition of three-dimensional images from SPECT. For the comparison, saline solutions containing ^{99m}Tc-DTPA tracer with different tonicity (hypertonic and normal saline) and droplet sizes (MMADs of 3.2 and 6.5 μm and span indices of 1.8 and 1.7, respectively) were aerosolized to six human subjects during tidal breathing. Using laser diffractometry, the span index was defined as the difference between 90 and 10% cumulative volumes, divided by volume mean diameter: span = $(Dv_{(90)} - Dv_{(10)})/Dv_{(50)}$. The hypertonic saline aerosols were expected to undergo hygroscopic growth as the droplets travel through the humid airways. Though, due to insufficient time for growth coupled with effect of mass transfer, the increase in aerodynamic diameter by small hypertonic saline droplets was expected by the authors to reach an intermediate size between 3.2 and 6.5 μm. Consequently, it would be expected to demonstrate a pulmonary deposition pattern intermediate to the smaller and bigger airways. Based on the work by Fleming et al. (1997), the lung images from SPECT were likewise subdivided into concentric shells as previously explained and the regional deposition of the particles in the lungs was determined according to the penetration index (P/C ratio). However, only deposition in the right lung was considered, since the image of the left lung may include confounding factors from the stomach and cardiac shadow.

In fact, the three-dimensional imaging technique proved to demonstrate a higher sensitivity than the planar scintigraphy. Not surprisingly, both techniques were able to detect the significant differences in penetration index that could be observed between the small normal saline and the large (both hypertonic and normal saline) droplets. However, the dynamic SPECT imaging was able to additionally identify significant differences in intermediate particle sizes being deposited in intermediate regions of the airways that could not be achieved by the two-dimensional scintigraphic method. More importantly, the study was able to demonstrate that smaller particles are deposited more peripherally in the lungs. The mean (±SEM) penetration indexes as measured by SPECT for small normal saline, small hypertonic saline, large normal saline and large hypertonic saline droplets were, respectively, 0.501 ± 0.043, 0.432 ± 0.022, 0.358 ± 0.024, and 0.338 ± 0.017. Interestingly, no

significant difference in regional pulmonary deposition was found between the different tonicities of large droplets. This finding may be related to the already central deposition of these larger aerodynamic particles, with little further hygroscopic effect to the large hypertonic saline aerosol.

A similar study has recently been published to confirm the deposition of small particles in the peripheral region of the lungs, following pulmonary administration using an Aeroliser® DPI device (Glover et al., 2008). Eight healthy volunteers were dosed with powder aerosols of mannitol radiolabelled with ^{99m}Tc complexed to Diethylene Triamine Pentaacetic Acid (DTPA) prepared by co-spray drying. The incorporation of radionuclide to mannitol did not present difference in particle sizes. This indicates the validity of using this radiolabelling method to determine the mannitol deposition in the lungs by measuring the radioactivity. The three different formulations evaluated presented particles with MMADs of 2.7, 3.6 and 5.4 μm and GSDs of 2.6, 2.4 and 2.7. The lungs of the human subjects were analyzed using SPECT and the images were divided into 10 concentric shells: central (5 innermost shells), peripheral (2 outermost shells) and intermediate (remaining 3 shells). An interesting finding from this study was that decreasing the particle aerodynamic diameter from 5.4 to 3.6 μm significantly increased the peripheral deposition. However, decreasing MMAD further from 3.6 to 2.7 μm did not improve significantly particle deposition in the lung periphery. With a greater deposition of the smaller particles more diffusively throughout the lungs consequently provided a greater lung dose. Alternatively, the deposition in the upper airways was significantly higher for bigger particles (>70%).

In addition, Glover and coworkers investigated an intersubject variation in total lung dose based on individual subject flow patterns and inspiratory airflow rate. With peak inhalation flow greater than 90 L/min for all patients, no correlation could be drawn since no difference in *in vitro* deposition was found between airflow rates of 60 and 100 L/min. Results of airflow rate and deposition patterns have been previously correlated, however using different DPI devices (Inhalator™) (Glover et al., 2006) or the same device with different airflow rate ranges (Meyer et al., 2004). Although a consistent polydispersity characteristic was observed for the three different formulations of mannitol powder, the results obtained in this investigation using a more reliable imaging tool (SPECT) for regional lung deposition helps to support the evidence that aerodynamically smaller particles deposit in the smaller airways.

While regional lung deposition of micronized aerosols is more frequently reported, the investigation of nanometer aerosols deposition in specific regions of the lungs is not available in the literature. Considering the late advances in nanotechnology, the regional dosimetry of nanoaerosols has been identified as a specific gap by the National Institute for Occupational Safety and Health (NIOSH, 2005). More recently, Ruzer and Apte discussed the difficulties related to available experimental techniques for assessment of local deposition of nanoparticles (i.e. particles ranging from 1 to 100 nm) in humans (Ruzer and Apte, 2010). The authors then go on to propose a potential method to be used for this purpose based on the unattached fraction of radon progeny. This marker forms naturally by decay of the inert radioactive gas radon and presents the smallest radioactive size, 1 nm. Through diffusion mechanism, this marker can deposit onto the surface of particles ranging from nanometer to micrometer dimensions and therefore has a potential for application in the regional dosimetry of nanoparticle aerosols. This approach has been previously used for determining extrathoracic deposition patterns in the human respiratory tract following nose- and mouth-breathing (Butterweck et al., 2001).

Nonetheless, a formulation of salbutamol with primary particles in the geometric nanosize range has been investigated for the local lung deposition (Bhavna et al., 2009). The Quasi-Elastic Light Scattering (QELS) results from this study showed that more than 70% of the particles prepared by spray-drying had a diameter smaller than 100 nm. The particle size results were confirmed by Scanning Electron Microscopy (SEM), which also demonstrated a well-defined round shaped morphology. The nanoparticles obtained were then compared to micronized particles of salbutamol in terms of aerodynamic diameter and regional deposition following inhalation with a Rotahaler® DPI device. The nano-salbutamol formulation presented an MMAD of 1.6 μm, with the discrepancy to the geometric diameter attributed to a potential aggregation due to interparticle adhesion in the dry state. Despite of that, the distribution of particle deposition in the Andersen Cascade Impactor showed that approximately 20% of the formulation presented aerodynamic diameter smaller than 150 nm. The MMAD of the micronized drug was approximately 3.1 μm. The healthy volunteers were trained to retain the breath for 10 s following deep inhalation and exhale into a collecting bag. Considering the diffusion mechanism related to ultrafine particles, an improvement in deposition of particles is expected with this breath-holding maneuver (Kim and Jaques, 2005). The planar scintigraphy imaging results, using the tracer ^{99m}Tc, showed a peripheral deposition of the nanoparticles greater than 2-fold higher than the micronized salbutamol and a minimal exhaled fraction (<1% of the emitted dose).

Similarly to the results obtained with humans, the studies in animals have presented the same evidence for the deposition of small particles in the lower (smaller) airways, despite the differences in the structure of their respiratory tract and breathing characteristics (nose versus mouth breathing) (Miller et al., 1993). Animal species studied include rodents, dogs, minipigs, and monkeys; and intraspecies variability has been reported to be similar to that of humans (Cheng et al., 2008; Schlesinger, 1985; Windt et al., 2010). Besides the scintigraphic techniques generally used for studies in humans, more recently a fluorescent imaging method has been introduced to study deposition patterns in lungs of animals (Yi et al., 2010).

Age is a determinant factor in the airway caliber of humans, with both increasing gradually from the newborn to the adult phase. Considering this fact, formulations developed for inhalation therapy based on adults may have a significant impact on their application to infants and young children. The relatively smaller airways of this subset of patients are a critical factor for the drug to reach the lower airways (Amirav et al., 2010; Schuepp et al., 2004b).

For this reason, some studies have investigated specifically the importance of aerosol formulations with smaller aerodynamic particle sizes to be delivered to children. In certain studies, the distinction in particle deposition is based solely on the difference in radioactivity observed in intra- and extrathoracic regions. Although they lack distinctive information on more specific pulmonary regions (e.g. terminal airway region), these investigations provide valuable data from a different viewpoint, in which they are based on differences in particle deposition between oropharyngeal (larger airways) and deep lung (lower airways). Comparing deposition in the lower versus the upper respiratory tract, budesonide droplets radiolabelled with ^{99m}Tc presented MMADs of 2.5 μm (GSD of 1.25) and 4.2 μm (GSD of 2.0) after nebulization with eFlow® and Pari LC Plus® nebulizers, respectively (Schuepp et al., 2004a). Using planar gamma scintigraphy to analyze six asymptomatic three-year old children, Schuepp and coworkers found that lung deposition was 36–38% and 5–8%, for children inhaling particles with MMADs of 2.5 and 4.2 μm, respectively. In a similar study, jet nebulizers were used to produce aerosols with MMADs of 3.6 and 7.7 μm (Mallol et al., 1996). With 20 asymptomatic cystic fibrosis patients, ages 3- to 24-months old, lung deposition of nebulized small particles was also greater than large particles. The ideal size of particles and best method of delivery; however, have not been clearly established in infants and young children.

6. Establishing clear relationships

The respiratory tract is a complex anatomical structure in which the upper airways gradually decrease in diameter down to the small dimensions of the terminal airways and alveoli. The *in vitro* determination of aerodynamic diameters has long been explored as a parameter to correlate regional lung deposition with *in vivo* studies. For the development of inhalation products, the use of cascade impactors highly benefits the fast screening of formulations. Hence, since the studies from Stahlhofen et al., in the late 1980s, the optimal particle sizes for inhalation products have been highly speculated. Consequently, rules-of-thumb have arisen. The most common one found in publications related to development of formulations for pulmonary delivery is that particles in the range of 1–5 μm are deposited in the deep lungs; while those larger than 10 μm are generally deposited in the oropharyngeal region and the particles smaller than 1 μm are exhaled (Chow et al., 2007; Haughney et al., 2010; Malcolmson and Embleton, 1998; Usmani, 2009). In an attempt to determine a more consistent *in vitro*/*in vivo* relationship, Newman and Chan have evaluated the results available in the literature for DPIs and pMDIs (Newman and Chan, 2008). Comparing the whole-lung deposition as a function of fine particle fraction, they found that the scattered data straddled the line of identity when particles were smaller than 3 μm. This may suggest an upper limit for particle size related to deposition in the deep lungs. So far, this finding in conjunction with the published data summarized in this review paper may be the best guide to predict deposition in the small airways, although it does not present a high level of accuracy, since other factors influence deposition (e.g. particle shape and degree of airway inflammation).

Just as it is important to define an upper limit of particle size distributed in various regions of the lung, it is also important to define the lower limit for each region. Considering the gradual, but not stepwise, decrease in the dimensions from the upper to the lower airways and the often polydispersed characteristic of orally inhaled products, it is reasonable to expect difficulties though in determining a specific cut off particle size range that translate into regional deposition in the lungs. One reason for that is the fact that the current available methods provide information on deposition via inertial impaction only, regardless of the other two significant mechanisms that can occur: sedimentation and diffusion (Mitchell and Nagel, 2003). Elutriation is the process by which particles are separated when moving upwards suspended in a fluid at a determined velocity. Elutriators have been developed to operate based on the principle of sedimentation; however they have not yet been widely applied to characterization of pharmaceutical formulations for inhalation therapy (Tillery and Buchan, 2002). Specifically for the diffusion mechanism, not only methods for characterization of aerosols are not available, but also dosimetry techniques are yet to be developed, as discussed earlier. The lack of information on the determination of aerodynamic particle sizes based on the three possible mechanisms of deposition may be the gap to determine more specific ranges of MMAD that correlates to regional deposition in the lungs. The late advances in *in vivo* experimental techniques, mainly related to three-dimensional imaging, have certainly developed towards meeting this need. Even though the optimal particle size range is yet to be defined, the reports available in the literature are evident about the deposition of smaller particles in the deep lungs, as opposed to deposition in the larger airways.

7. Conclusions

Despite the limitations in early imaging techniques used to determine particle deposition in specific zones of the lungs, the technological advances in imaging techniques are gradually improving the capability of differentiating the deposition patterns of particles with increasingly smaller differences in aerodynamic dimensions. With the advances in SPECT and PET, more confirmatory studies are being reported of the evidence of deposition of small particles in the smaller airways, as opposed to deposition in the larger airways. Nonetheless, the imaging techniques can also be used for less specific studies in the respiratory tract by comparing extrathoracic (upper airways: oropharyngeal cavity) versus intrathoracic (lower airways: lower trachea, bronchi, bronchioles and alveoli) particle deposition. This has been more frequently reported in studies with children.

The urge to establish clear relationships between *in vitro* aerodynamic determination and *in vivo* particle deposition has led to comparisons between fine particle fraction and total lung deposition of particles. Results based on impaction studies indicate that particles smaller than 3 μm are more likely to deposit in the deep lungs. However, there is a lack of information about the regional lung deposition of particles affected by non-impaction mechanisms (e.g. sedimentation and diffusion), largely due to lack of applicable *in vitro* and *in vivo* experimental techniques; however, there is sufficient evidence reported in the literature showing that smaller aerodynamic particles deposit in the lower portion of the respiratory tract where the airways are gradually smaller. As imaging techniques advance, investigation of how particle size, shape, charge, and composition affect deposition and movement through both the airway and the lung's mucous gel layer will be required in order to optimize drug delivery through the inhaled route.

References

Amirav, I., Newhouse, M.T., Minocchieri, S., Castro-Rodriguez, J.A., Schuepp, K.G., 2010. Factors that affect the efficacy of inhaled corticosteroids for infants and young children. J. Allergy Clin. Immunol. 125, 1206–1211.

Balashazy, I., Alfoldy, B., Molnar, A.J., Hofmann, W., Szoke, I., Kis, E., 2007. Aerosol drug delivery optimization by computational methods for the characterization of total and regional deposition of therapeutic aerosols in the respiratory system. Curr. Comput. Aided Drug Des. 3, 13–32.

Berridge, M.S., Heald, D.L., Lee, Z., 2003. Imaging studies of biodistribution and kinetics in drug development. Drug Dev. Res. 59, 208–226.

Berridge, M.S., Lee, Z., Heald, D.L., 2000a. Pulmonary distribution and kinetics of inhaled [c-11]triamcinolone acetonide. J. Nucl. Med. 41, 1603–1611.

Berridge, M.S., Lee, Z.H., Heald, D.L., 2000b. Regional distribution and kinetics of inhaled pharmaceuticals. Curr. Pharm. Des. 6, 1631–1651.

Bhavna, Ahmad, F.J., Mittal, G., Jain, G.K., Malhotra, G., Khar, R.K., Bhatnagar, A., 2009. Nano-salbutamol dry powder inhalation: a new approach for treating bronchoconstrictive conditions. Eur. J. Pharm. Biopharm. 71, 282–291.

Brand, P., Haussinger, K., Meyer, T., Scheuch, G., Schulz, H., Selzer, T., Heyder, J., 1999. Intrapulmonary distribution of deposited particles. J. Aerosol Med. Depos. Clear. Eff. Lung 12, 275–284.

Butterweck, G., Vezzu, G., Schuler, C., Muller, R., Marsh, J.W., Thrift, S., Birchall, A., 2001. *In vivo* measurement of unattached radon progeny deposited in the human respiratory tract. Radiat. Prot. Dosim. 94, 247–250.

Carroll, N., Elliot, J., Morton, A., James, A., 1993. The structure of large and small airways in nonfatal and fatal asthma. Am. Rev. Respir. Dis. 147, 405–410.

Chan, H.K., Daviskas, E., Eberl, S., Robinson, M., Bautovich, G., Young, I., 1999. Deposition of aqueous aerosol of technetium-99m diethylene triamine penta-acetic acid generated and delivered by a novel system (AER_X) in healthy subjects. Eur. J. Nucl. Med. 26, 320–327.

Chan, H.K., Eberl, S., Daviskas, E., Constable, C., Young, I., 2002. Changes in lung deposition of aerosols due to hygroscopic growth: a fast SPECT study. J. Aerosol Med. Depos. Clear. Eff. Lung 15, 307–311.

Cheng, Y.S., Irshad, H., Kuehl, P., Holmes, T.D., Sherwood, R., Hobbs, C.H., 2008. Lung deposition of droplet aerosols in monkeys. Inhal. Toxicol. 20, 1029–1036.

Chow, A.H.L., Tong, H.H.Y., Chattopadhyay, P., Shekunov, B.Y., 2007. Particle engineering for pulmonary drug delivery. Pharm. Res. 24, 411–437.

Chrystyn, H., 2001. Methods to identify drug deposition in the lungs following inhalation. Br. J. Clin. Pharmacol. 51, 289–299.

Clark, A., Kuo, M.C., Newman, S., Hirst, P., Pitcairn, G., Pickford, M., 2008. A comparison of the pulmonary bioavailability of powder and liquid aerosol formulations of salmon calcitonin. Pharm. Res. 25, 1583–1590.

Coates, A.L., Green, M., Leung, K., Chan, J., Ribeiro, N., Louca, E., Ratjen, F., Charron, M., Tservistas, M., Keller, M., 2008. Rapid pulmonary delivery of inhaled tobramycin for pseudomonas infection in cystic fibrosis: a pilot project. Pediatr. Pulmonol. 43, 753–759.

Corren, J., Tashkin, D.R., 2003. Evaluation of efficacy and safety of flunisolide hydrofluoroalkane for the treatment of asthma. Clin. Ther. 25, 776–798.

Crowder, T.M., Rosati, J.A., Schroeter, J.D., Hickey, A.J., Martonen, T.B., 2002. Fundamental effects of particle morphology on lung delivery: predictions of Stokes' law and the particular relevance to dry powder inhaler formulation and development. Pharm. Res. 19, 239–245.

Cryan, S.-A., Sivadas, N., Garcia-Contreras, L., 2007. *In vivo* animal models for drug delivery across the lung mucosal barrier. Adv. Drug Deliv. Rev. 59, 1133–1151.

Darquenne, C., Prisk, G.K., 2008. Deposition of inhaled particles in the human lung is more peripheral in lunar than in normal gravity. Eur. J. Appl. Physiol. 103, 687–695.

Davis, S.S., Hardy, J.G., Newman, S.P., Wilding, I.R., 1992. Gamma-scintigraphy in the evaluation of pharmaceutical dosage forms. Eur. J. Nucl. Med. 19, 971–986.

de Boer, A.H., Gjaltema, D., Hagedoorn, P., Frijlink, H.W., 2002. Characterization of inhalation aerosols: a critical evaluation of cascade impactor analysis and laser diffraction technique. Int. J. Pharm. 249, 219–231.

Dolovich, M., Labiris, R., 2004. Imaging drug delivery and drug responses in the lung. Proc. Am. Thorac. Soc. 1, 329–337.

Dolovich, M.A., 2000. Influence of inspiratory flow rate, particle size, and airway caliber on aerosolized drug delivery to the lung. Respir. Care 45, 597–608.

Dolovich, M.B., 2009. ^{18}F-fluorodeoxyglucose positron emission tomographic imaging of pulmonary functions, pathology, and drug delivery. Proc. Am. Thorac. Soc. 6, 477–485.

Eberl, S., Chan, H.K., Daviskas, E., 2006. SPECT imaging for radioaerosol deposition and clearance studies. J. Aerosol Med. Depos. Clear. Eff. Lung 19, 8–20.

Eberl, S., Chan, H.K., Daviskas, E., Constable, C., Young, I., 2001. Aerosol deposition and clearance measurement: a novel technique using dynamic SPET. Eur. J. Nucl. Med. 28, 1365–1372.

Edwards, D.A., Hanes, J., Caponetti, G., Hrkach, J., BenJebria, A., Eskew, M.L., Mintzes, J., Deaver, D., Lotan, N., Langer, R., 1997. Large porous particles for pulmonary drug delivery. Science 276, 1868–1871.

Emmen, H.H., Hoogendijk, E.M.G., Klopping-Ketelaars, W.A.A., Muijser, H., Duistermaat, E., Ravensberg, J.C., Alexander, D.J., Borkhataria, D., Rusch, G.M., Schmit, B., 2000. Human safety and pharmacokinetics of the CFC alternative propellants HFC 134a (1,1,1,2-tetrafluoroethane) and HFD 227 (1,1,1,2,3,3,3-heptafluoropropane) following whole-body exposure. Regul. Toxicol. Pharmacol. 32, 22–35.

Farr, S.J., 1996. The physico-chemical basis of radiolabelling metered dose inhalers with Tc-99m. J. Aerosol Med. Depos. Clear. Eff. Lung 9, S27–S36.

Finlay, W.H., 2001. Particle deposition in the respiratory tract. In: Finlay, W.H. (Ed.), The Mechanics of Inhaled Pharmaceutical Aerosols: An Introduction. Academic Press, San Diego, CA, pp. 119–174.

Fleming, J.S., Hashish, A.H., Conway, J.H., HartleyDavies, R., Nassim, M.A., Guy, M.J., Coupe, J., Holgate, S.T., Moore, E., Bailey, A.G., Martonen, T.B., 1997. A technique for simulating radionuclide images from the aerosol deposition pattern in the airway tree. J. Aerosol Med. Depos. Clear. Eff. Lung 10, 199–212.

Glover, W., Chan, H.-K., Eberl, S., Daviskas, E., Verschuer, J., 2008. Effect of particle size of dry powder mannitol on the lung deposition in healthy volunteers. Int. J. Pharm. 349, 314–322.

Glover, W., Chan, H.K., Eberl, S., Daviskas, E., Anderson, S., 2006. Lung deposition of mannitol powder aerosol in healthy subjects. J. Aerosol Med. Depos. Clear. Eff. Lung 19, 522–532.

Gonda, I., 2004. Targeting by deposition. In: Hickey, A.J. (Ed.), Pharmaceutical Inhalation Aerosol Technology. Marcel Dekker, Inc., New York, NY, USA, pp. 65–88.

Guenther, K.J., Yoganathan, S., Garofalo, R., Kawabata, T., Strack, T., Labiris, R., Dolovich, M., Chirakal, R., Valliant, J.F., 2006. Synthesis and *in vitro* evaluation of ^{18}F- and ^{19}F-labeled insulin: a new radiotracer for PET-based molecular imaging studies. J. Med. Chem. 49, 1466–1474.

Gurses, B.K., Smaldone, G.C., 2003. Effect of tubing deposition, breathing pattern, and temperature on aerosol mass distribution measured by cascade impactor. J. Aerosol Med. Depos. Clear. Eff. Lung 16, 387–394.

Haughney, J., Price, D., Barnes, N.C., Virchow, J.C., Roche, N., Chrystyn, H., 2010. Choosing inhaler devices for people with asthma: current knowledge and outstanding research needs. Respir. Med. 104, 1237–1245.

Hinds, W.C., 1999. Respiratory deposition. In: Hinds, W.C. (Ed.), Aerosol Technology: Properties, Behavior, and Measurement of Airborne Particles. , 2nd ed. Wiley, New York, pp. 233–259.

Iozzo, P., Osman, S., Glaser, M., Knickmeier, M., Ferrannini, E., Pike, V.W., Camici, P.G., Law, M.P., 2002. *In vivo* imaging of insulin receptors by PET: preclinical evaluation of iodine-125 and iodine-124 labelled human insulin. Nucl. Med. Biol. 29, 73–82.

Jaafar-Maalej, C., Andrieu, V., Elaissari, A., Fessi, H., 2009. Assessment methods of inhaled aerosols: technical aspects and applications. Expert Opin. Drug Deliv. 6, 941–959.

Kim, C.S., Jaques, P.A., 2005. Total lung deposition of ultrafine particles in elderly subjects during controlled breathing. Inhal. Toxicol. 17, 387–399.

Kleinstreuer, C., Zhang, Z., Donohue, J.F., 2008. Targeted drug-aerosol delivery in the human respiratory system. Annu. Rev. Biomed. Eng. 10, 195–220.

Koehler, E., Sollich, V., Schuster-Wonka, R., Huehnerbein, J., 2003. Lung deposition in cystic fibrosis patients using an ultrasonic or a jet nebulizer. J. Aerosol Med. 16, 37–46.

Labiris, N.R., Dolovich, M.B., 2003. Pulmonary drug delivery. Part II: The role of inhalant delivery devices and drug formulations in therapeutic effectiveness of aerosolized medications. Br. J. Clin. Pharmacol. 56, 600–612.

Leach, C.L., Davidson, P.J., Boudreau, R.J., 1998. Improved airway targeting with the CFC-free HFA-beclomethasone metered-dose inhaler compared with CFC-beclomethasone. Eur. Respir. J. 12, 1346–1353.

Leach, C.L., Davidson, P.J., Hasselquist, B.E., Boudreau, R.J., 2005. Influence of particle size and patient dosing technique on lung deposition of HFA-beclomethasone from a metered dose inhaler. J. Aerosol Med. Depos. Clear. Eff. Lung 18, 379–385.

Malcolmson, R.J., Embleton, J.K., 1998. Dry powder formulations for pulmonary delivery. Pharm. Sci. Technol. Today 1, 394–398.

Mallol, J., Rattray, S., Walker, G., Cook, D., Robertson, C.F., 1996. Aerosol deposition in infants with cystic fibrosis. Pediatr. Pulmonol. 21, 276–281.

Martin, A.R., Thompson, R.B., Finlay, W.H., 2008. MRI measurement of regional lung deposition in mice exposed nose-only to nebulized superparamagnetic iron oxide nanoparticles. J. Aerosol Med. Pulm. Drug Deliv. 21, 335–341.

Martin, R.J., 2002. Therapeutic significance of distal airway inflammation in asthma. J. Allergy Clin. Immunol. 109, S447–S460.

Martonen, T., Fleming, J., Schroeter, J., Conway, J., Hwang, D., 2003. *In silico* modeling of asthma. Adv. Drug Deliv. Rev. 55, 829–849.

Martonen, T., Isaacs, K., Hwang, D.M., 2005. Three-dimensional simulations of airways within human lungs. Cell Biochem. Biophys. 42, 223–249.

Martonen, T.B., Schroeter, J.D., Fleming, J.S., 2007. 3D *in silico* modeling of the human respiratory system for inhaled drug delivery and imaging analysis. J. Pharm. Sci. 96, 603–617.

Meyer, T., Brand, P., Ehlich, H., Kobrich, R., Meyer, G., Riedinger, F., Sommerer, K., Weuthen, T., Scheuch, G., 2004. Deposition of foradil P in human lungs: comparison of *in vitro* and *in vivo* data. J. Aerosol Med. Depos. Clear. Eff. Lung 17, 43–49.

Meyer, T., Muellinger, B., Sommerer, K., Scheuch, G., Brand, P., Beckmann, H., Haeussinger, K., Weber, N., Siekmeier, R., 2003. Pulmonary deposition of monodisperse aerosols in patients with chronic obstructive pulmonary disease. Exp. Lung Res. 29, 475–484.

Miller, F.J., Mercer, R.R., Crapo, J.D., 1993. Lower respiratory-tract structure of laboratory-animals and humans – dosimetry implications. Aerosol Sci. Technol. 18, 257–271.

Mitchell, J.P., Nagel, M.W., 2003. Cascade impactors for the size characterization of aerosols from medical inhalers: their uses and limitations. J. Aerosol Med. Depos. Clear. Eff. Lung 16, 341+.

Moller, W., Felten, K., Meyer, G., Meyer, P., Seitz, J., Kreyling, W.G., 2009a. Corrections in dose assessment of Tc-99m radiolabeled aerosol particles targeted to central human airways using planar gamma camera imaging. J. Aerosol Med. Pulm. Drug Deliv. 22, 45–54.

Moller, W., Meyer, G., Scheuch, G., Kreyling, W.G., Bennett, W.D., 2009b. Left-to-right asymmetry of aerosol deposition after shallow bolus inhalation depends on lung ventilation. J. Aerosol Med. Pulm. Drug Deliv. 22, 333–339.

Newman, S., Malik, S., Hirst, P., Pitcairn, G., Heide, A., Pabst, J., Dinkelaker, A., Fleischer, W., 2002. Lung deposition of salbutamol in healthy human subjects from the MAGhaler dry powder inhaler. Respir. Med. 96, 1026–1032.

Newman, S.P., 1993. Scintigraphic assessment of therapeutic aerosols. Crit. Rev. Ther. Drug Carrier Syst. 10, 65–109.

Newman, S.P., Chan, H.K., 2008. *In vitro*/*in vivo* comparisons in pulmonary drug delivery. J. Aerosol Med. Pulm. Drug Deliv. 21, 77–84.

Newman, S.P., Pitcairn, G.R., Hirst, P.H., Rankin, L., 2003. Radionuclide imaging technologies and their use in evaluating asthma drug deposition in the lungs. Adv. Drug Deliv. Rev. 55, 851–867.

Newman, S.P., Wilding, I.R., 1999. Imaging techniques for assessing drug delivery in man. Pharm. Sci. Technol. Today 2, 181–189.

NIOSH, 2005. Strategic Plan for NIOSH Nanotechnology Research and Guidance – Filling the Knowledge Gap. Nanotechnology Research Program, Centers for Disease Control and Prevention, National Institute for Occupational Safety and Health, p. 103.

Pickering, H., Pitcairn, G.R., Hirst, P.H., Bacon, R.E., Newman, S.P., Affrime, M.B., Marino, M., 2000. Regional lung deposition of a technetium 99m-labeled formulation of mometasone furoate administered by hydrofluoroalkane 227 metered-dose inhaler. Clin. Ther. 22, 1483–1493.

Pilcer, G., Amighi, K., 2010. Formulation strategy and use of excipients in pulmonary drug delivery. Int. J. Pharm. 392, 1–19.

Pilcer, G., Vanderbist, F., Amighi, K., 2008. Correlations between cascade impactor analysis and laser diffraction techniques for the determination of the particle size of aerosolised powder formulations. Int. J. Pharm. 358, 75–81.

Rostami, A.A., 2009. Computational modeling of aerosol deposition in respiratory tract: a review. Inhal. Toxicol. 21, 262–290.

Ruzer, L.S., Apte, M.G., 2010. Unattached radon progeny as an experimental tool for dosimetry of nanoaerosols: proposed method and research strategy. Inhal. Toxicol. 22, 760–766.

Sangwan, S., Condos, R., Smaldone, G.C., 2003. Lung deposition and respirable mass during wet nebulization. J. Aerosol Med. Depos. Clear. Eff. Lung 16, 379–386.

Schlesinger, R.B., 1985. Comparative deposition of inhaled aerosols in experimental-animals and humans – a review. J. Toxicol. Environ. Health 15, 197–214.

Schmekel, B., Hedenstrom, H., Hedenstierna, G., 2002. Deposition of terbutaline in the large or small airways: a single-center pilot study of ventilation-perfusion distributions and airway tone. Curr. Ther. Res. Clin. Exp. 63, 536–548.

Schuepp, K.G., Devadason, S., Roller, C., Wildbaber, J.H., 2004a. A complementary combination of delivery device and drug formulation for inhalation therapy in preschool children. Swiss Med. Wkly. 134, 198–200.

Schuepp, K.G., Straub, D., Moller, A., Wildhaber, J.H., 2004b. Deposition of aerosols in infants and children. J. Aerosol Med. Depos. Clear. Eff. Lung 17, 153–156.

Shekunov, B.Y., Chattopadhyay, P., Tong, H.H.Y., Chow, A.H.L., 2007. Particle size analysis in pharmaceutics: principles, methods and applications. Pharm. Res. 24, 203–227.

Shoyele, S.A., Cawthome, S., 2006. Particle engineering techniques for inhaled biopharmaceuticals. Adv. Drug Deliv. Rev. 58, 1009–1029.
Smith, J.R.H., Bailey, M.R., Etherington, G., Shutt, A.L., Youngman, M.J., 2008. Effect of particle size on slow particle clearance from the bronchial tree. Exp. Lung Res. 34, 287–312.
Stahlhofen, W., Rudolf, G., James, A.C., 1989. Intercomparison of experimental regional aerosol deposition data. J. Aerosol Med. 2, 285–308.
Thorsson, L., Kenyon, C., Newman, S.P., Borgstrom, L., 1998. Lung deposition of budesonide in asthmatics: a comparison of different formulations. Int. J. Pharm. 168, 119–127.
Tillery, M., Buchan, R., 2002. Determination of large aerosol particle size by elutriation. Appl. Occup. Environ. Hyg. 17, 717–722.
UNEP, 1987. The Montreal Protocol on Substances that Deplete the Ozone Layer. United Nations Environment Programme, Nairobi, p. 54.
Usmani, O.S., 2009. Delivery of drugs to the airways. In: Usmani, O.S. (Ed.), Lung Biol Health Dis. , pp. 143–161.
Usmani, O.S., Biddiscombe, M.F., Barnes, P.J., 2005. Regional lung deposition and bronchodilator response as a function of beta(2)-agonist particle size. Am. J. Respir. Crit. Care Med. 172, 1497–1504.
van Waarde, A., Maas, B., Doze, P., Slart, R.H., Frijlink, H.W., Vaalburg, W., Elsinga, P.H., 2005. Positron emission tomography studies of human airways using an inhaled beta-adrenoceptor antagonist, S-C-11-CGP 12388. Chest 128, 3020–3027.
Vanden Burgt, J.A., Busse, W.W., Martin, R.J., Szefler, S.J., Donnell, D., 2000. Efficacy and safety overview of a new inhaled corticosteroid. QVAR (hydrofluoroalkane-beclomethasone extrafine inhalation aerosol), in asthma. J. Allergy Clin. Immunol. 106, 1209–1226.
Visser, T.J., van Waarde, A., Doze, P., Elsinga, P.H., van der Mark, T.W., Kraan, J., Ensing, K., Vaalburg, W., 1998. Characterisation of beta(2)-adrenoceptors, using the agonist [C-11]formoterol and positron emission tomography. Eur. J. Pharmacol. 361, 35–41.
Windt, H., Kock, H., Runge, F., Hubel, U., Koch, W., 2010. Particle deposition in the lung of the gottingen minipig. Inhal. Toxicol. 22, 828–834.
Xie, Y.Y., Zeng, P.Y., Siegel, R.A., Wiedmann, T.S., Hammer, B.E., Longest, P.W., 2010. Magnetic deposition of aerosols composed of aggregated superparamagnetic nanoparticles. Pharm. Res. 27, 855–865.
Yi, D., Price, A., Panoskaltsis-Mortari, A., Naqwi, A., Wiedmann, T.S., 2010. Measurement of the distribution of aerosols among mouse lobes by fluorescent imaging. Anal. Biochem. 403, 88–93.
Zanen, P., Go, L.T., Lammers, J.W.J., 1995. The optimal particle-size for parasympathicolytic aerosols in mild asthmatics. Int. J. Pharm. 114, 111–115.
Zanen, P., Go, L.T., Lammers, J.W.J., 1996. Optimal particle size for beta(2) agonist and anticholinergic aerosols in patients with severe airflow obstruction. Thorax 51, 977–980.
Zanen, P., Go, L.T., Lammers, J.W.J., 1998. The efficacy of a low-dose, monodisperse parasympathicolytic aerosol compared with a standard aerosol from a metered-dose inhaler. Eur. J. Clin. Pharmacol. 54, 27–30.
Zeng, X.M., Martin, G.P., Marriott, C., 2001. Medicinal aerosols. In: Zeng, X.M., Martin, G.P., Marriott, C. (Eds.), Particulate Interactions in Dry Powder Formulations for Inhalation. Taylor & Francis, New York, NY, pp. 65–102.